CoFee-L: A model of animal displacement in large groups combining Cohesion maintenance, Feeding area search and transient Leadership.

Nikita Gavrilitchenko (n.gavrilitchenko@uliege.be)
University of Liège
Eva Gazagne
University of Liège
Nicolas Vandewalle
University of Liège
Johann Delcourt
University of Liège
Alain Hambuckers
University of Liège

Research Article

Keywords: Mechanistic modelling, Mean squared displacement, Seed dispersal, Collective movement, Individual based model

Posted Date: June 22nd, 2022

DOI: https://doi.org/10.21203/rs.3.rs-1758343/v1

Version of Record: A version of this preprint was published at Animals on September 14th, 2022. See the published version at https://doi.org/10.3390/ani12182412.

CoFee-L: A model of animal displacement in large groups combining Cohesion maintenance, Feeding area search and transient Leadership

Nikita GAVRILITCHENKO

» Corresponding author
» Department of Biology, Ecology and Evolution, Faculty of Science, University of Liege, Quai Van Beneden 22, 4020 Liège, Belgium
» n.gavrilitchenko@uliege.be

Eva GAZAGNE

» University of Liege, Belgium
» evagazagne@live.fr

Nicolas VANDEWALLE

» University of Liege, Belgium
» nvandewalle@uliege.be

Johann DELCOURT

» University of Liege, Belgium
» johann.delcourt@uliege.be

Alain HAMBUCKERS

» University of Liege, Belgium
» alain.hambuckers@uliege.be

ABSTRACT

BACKGROUND

In the current context of climate change and intensive anthropization of natural environments, the preservation of ecosystems is a matter of great importance. In the tropics, the conservation of tree species is closely linked to that of animals. A large proportion of tree species is zoochore and needs animals, mainly vertebrates, to disperse their seeds in order to increase their chances of survival. Being able to predict the movement of animals is therefore an important skill. Lots of research exists on the subject, but it has always focused on particular characteristics of collective behavior. In contrast to previous studies, we included the concepts of Cohesion maintenance, Feeding area search and transient Leadership in a single model, CoFee-L.

METHODS

We tested CoFee-L to simulate the movement of a wild-ranging troop of primates belonging to the species *Macaca leonina* in a nature reserve of Thailand. We analyzed this methodology by statistical physics tools (mean squared displacement) and we characterized the simulated trajectories by histograms and χ^2 for the step length and turning angle distributions sampled at the same frequency as the collection of field observations.

RESULTS

CoFee-L allowed us to reproduce the physical properties of the troop's centre of mass trajectory, as well as the step length and angle distributions of the field data. Moreover, CoFee-L is able to produce trajectories looking like correlated random walks or levy walks depending of the parametrisation.

CONCLUSIONS

We created a model, CoFee-L, which allowed us to simulate the movement of a group of vertebrates taking into account not only the movement and individual characteristics of each member, but this also independently of the group size. The parameterisation of CoFee-L was rather simple, as it was sufficient to fix a set of parameters easily observable in the field (number of individuals, size of the study site, duration of monitoring, duration of foraging, distance between individuals and maximum spread of the group) and then to adjust the values of 4 parameters which have biological meaning (personal information, exploration of the study site, speed of movement and tendency to do a levy walk).

KEYWORDS

Mechanistic modelling – Mean squared displacement – Seed dispersal – Collective movement – Individual based model

BACKGROUND

The understanding and the description of animal movements is challenging in the field of conservation, particularly for the design of the conservation areas. The reduction of the surfaces, devoted to wildlife in benefit to human activities, and the degradation of the environmental quality, limit the availability of resources and constrain animals in smaller areas. Either these animals are able to adapt their behaviour by exploitation of the remaining or new resources [1] or finally their local population goes extinct [2]. Another challenge, in tropical areas, is that a large proportion of tree species is zoochore and needs animals, mainly vertebrates, to disperse their seeds. The seed dispersal, i.e. the movement of seeds away from their parent plant, helps the trees escape their specific pathogens which

accumulate in their vicinity (e.g. [3]) and may provide opportunities to reach new suitable areas in case of changing environmental conditions, notably in connection with climate change. Thus, the conservation of the tree species in the tropics is tightly linked to that of animals. Unfortunately, tree species conservation is not considered so urgent because they are long-living being and their local extinction is a process slower than in animals. Considering the effect of climate change, repeatedly censused plots in the Andes highlighted thermophilization, i.e. the upward shifts of lowland, from warmer areas tree species, a phenomenon observed elsewhere in the tropics [4] or in mountains of temperate countries [5]. Shifts are also perceptible in lowlands at high latitudes [6]. Beyond observational studies, understanding or predicting the consequences of climate change on plant species could be inferred using modelling of past, present and future vegetation and plant species distribution and growth. The most often, this is done with species distribution models and with dynamic vegetation models. However, the projections rely on the implicit assumption of unlimited dispersal of the diaspores which is most often unrealistic. Modelling approaches need to be improved by including seed dispersal processes and thus animal movement patterns [7].

Models simulating the movement of a group of individual animals have to be upgraded and combined with the processes of seed transport and deposition to simulate seed dispersal kernels, i.e. the frequency distribution of dispersed seeds relative to distance from parent plants. The features of collective animal movements have been intensively studied with individual based models [8-10], which consider distinctly each individual interacting with its nearest neighbours to predict the individual trajectories. Combined together, those features should allow to simulate realistic collective movements. The first important characteristic that can be highlighted in collective animal movements is the existence of interactions between individuals [11]. The Vicsek's model, considering animals and micro-organisms as self-propelled particles converting the energy of their environment into directed movement, simulates basic movement behaviours and clustering of a gregarious animal [12]. In this

model, individual movements tend to be correlated with that of their neighbours: at each update step, the orientation of each particle in the system is modified as a function of the average orientation of the neighbouring particles. Although Vicsek's model is useful because its minimalism eases the analysis of its predictions, it lacks of biological realism. Particles do not avoid collisions nor show attraction to each other's, whereas the fact that animals tend to keep a minimum distance from each other's and align with their neighbours is a behaviour frequently observed in nature [13, 14]. New approaches have been developed that focus on the aggregation behaviour encountered in biological systems, based on local repulsions, alignment and attraction tendencies between individuals [9, 15-19]. These models are generally based on two rules: (1) at all times, individuals try to maintain a minimum distance between themselves and (2) if individuals do not perform an avoidance manoeuvre, i.e. do not try to move away from one or more individuals, they tend to be attracted to other individuals to avoid isolation and align themselves according to their neighbours. In order to maintain cohesion during locomotion, gregarious animals need however to make collective decisions [20, 21]. The second important feature affecting the collective movements is the interaction between individuals and their environment. Many species form complex societies with several levels of communities [22-25], and the integration of hierarchy allows improvement of realism of animal movement models when it comes to collective decision-making [26, 27]. However, the initiation of a movement may in some cases not be correlated with the level of hierarchy [28]. The leader is not necessarily permanent; he is in fact very often a leader more by its spatial location than its hierarchical dominant-dominated status.

Our objective was then to build and validate a new model (CoFee-L) based on the concepts of statistical physics describing the movements of animals belonging to large groups. We considered together cohesion, i.e. the trade-off between distance among individuals and group dispersal, random behaviour in search of food resources, knowledge of the habitat and social organization, i.e. that the individual closest of food becomes leader and attracts its congeners until the food was consumed. In

contrast to previous studies, the separate concepts they developed are included in the CoFee-L in order to come as close as possible to reality. As data for validation, we recorded the movements of a troop of ca. 140 primates belonging to the species *Macaca leonina* in the wild in a nature reserve of Thailand.

METHODS

Site

The study took place in the vicinity of the Sakaerat Environmental Research Station, a research station belonging to the Sakaerat Biosphere Reserve, 300km north-east of Bangkok, Thailand (14°26' to 14°32'N; 101°50' to 101°57'E). The reserve has an area of 80 sq. km with altitude ranging between 250 and 762m asl. It is covered by dry evergreen forest (53.4%), dry Dipterocarpaceae forest (14.8%), old growth forest plantations dominated by *Eucalyptus camaldulensis* and *Acacia mangium* (21.4%), grassland (6.1%), agroforestry (2.6%), bamboo groves (1.5%) and cultures (0.2%). The climate is of typically monsoonal character with a hot-wet season between May and October, a cold-dry season between November and February and a hot-dry season between March and April. The mean annual temperature is 25.6°C and the mean annual rainfall in the region is 1200mm (Thai Institute of Scientific and Technological Research, 2017).

Field observations

The group of interest was a troop of *Macaca leonina* (Blyth 1863), habituated to human observer and followed in order to study principally their space-use, foraging strategies and seed dispersal effectiveness in a degraded habitat [1, 29-31]. The troop included between 128 and 153 individuals with 11 to 15 adult males, 41 to 48 adult females and 76 to 90 juveniles in the course of monitoring period between February 2017 and May 2020. It occupied a home-range of 599 ha covered with 78%

of dry evergreen forest and with 22% of plantations. The troop was followed during several field work from sunrise to sunset during ca. 7 ensuing days per month (126 complete days and 35 days interrupted by troop losses, inclement weather, etc.), recording the position of the observer every minute with a standard field GPS. It is supposed that the observer occupied the centre of mass (CM) of the troop for the subsequent analysis. The daily trajectories of the troop were 2,151 ± 497m, regardless of the observation period.

When the troop stopped at a location and individuals fed for more than 10 minutes, the zone was considered as a feeding area (FA) and an average of the fruiting score for each species present was calculated to characterise the abundance of the FA. The fruiting score P_{sm} of species s for month m is a monthly estimate of fruit production that was made on a sample of referenced trees scattered in the primate home-range by visually scoring the fructification intensity (no fruits in the canopy: 0; fruits in 1 to 25 % of the canopy: 1; fruits in 26 to 50% of the canopy: 2; fruits in 51 to 75% of the canopy: 3; fruits in 76 to 100% of the canopy: 4). The more a FA is filled with trees with a large P_{sm}, the more abundant the FA. In order to characterize the monthly food availability in the study site, and thus to determine periods of food scarcity, a fruit availability index (FAI) was associated with each tree species present in the area [32]. To calculate this index, the following formula was used:

$$FAI_m = \Sigma_s D_s \overline{B}_s \overline{P}_{sm}$$

where D_s is the density of species s (stem/ha), $\overline{B}_s$ is the mean basal area of species s (m^2/ha) and $\overline{P}_{sm}$ is the average fruiting score of species s for month m.

Trajectory analysis

The animal moves were characterized with the mean squared displacement (MSD). Considering a particle moving in a two-dimensional space, its trajectory can be divided into N consecutives positions recorded with a constant step time Δt during a time period $T = (N-1)\Delta t$. The MSD measures the

deviation of a particle's position over time in relation to an initial position and is defined (discretely) such that:

$$\bar{\rho}_\tau = \frac{1}{N-\tau}\sum_{i=1}^{N-\tau} l_{i,i+\tau}^2\,, \quad \tau = 1, \dots, N-1$$

where $l_{i,i+\tau}$ is the distance between point *i* and point *i+*τ [33]. Since the number of data pairs decreases as τ increases, the uncertainty of the MSD calculation increases. Therefore, τ is usually limited to less than a quarter of the total number of data points (Saxton's rule) [34].

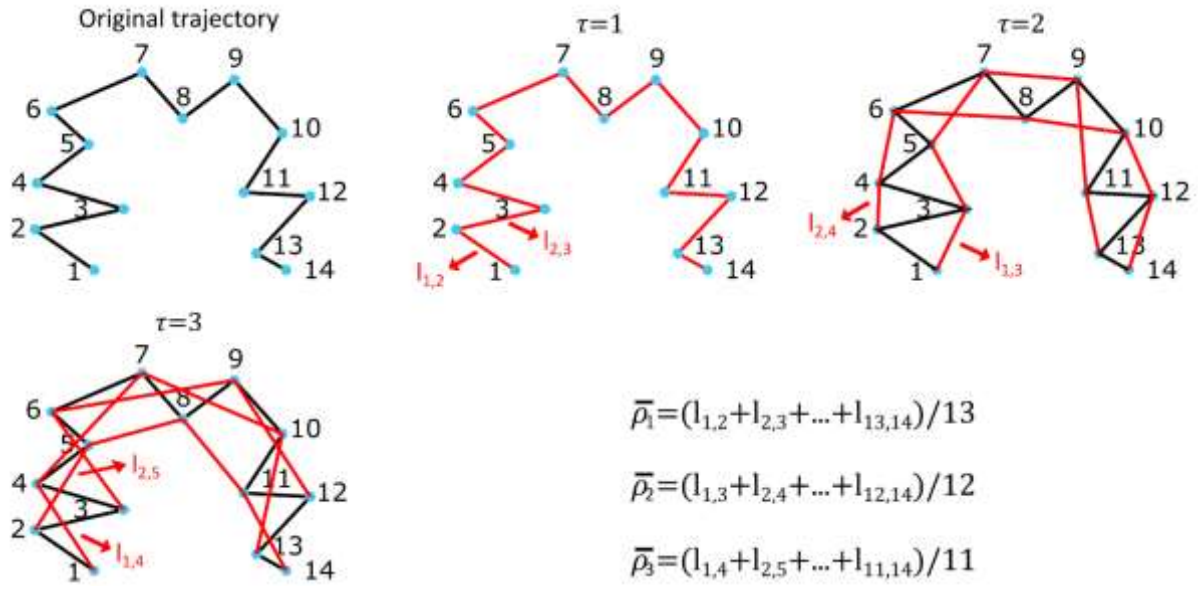

Fig. 1 – Schematic representation of the mean squared displacement (MSD) calculation for a trajectory comprising 14 points. The MSD is calculated up to τ=3, according to Saxton's rule [34].

The MSD is a fundamental tool as it not only gives an idea of the part of the system explored by a walker but also identifies the type of diffusion one is dealing with [35, 36]. In fact, a particle propagating

solely due to diffusion (Brownian motion) will result in a linear dependence of the MSD on time, while a non-linear dependence will be a signature of an anomalous diffusion. The key parameter is the value of α observed in the proportionality relation:

$$\bar{\rho}_\tau \propto \tau^\alpha.$$

In the case of $\alpha = 0$, we are simply faced with a *stationary* process where no movement is carried out during the observation period. For $0 < \alpha < 1$, the regime is called *subdiffusive* because the MSD increases less rapidly than in the case of a classical diffusion. This kind of situation can be encountered in motion models where there are waiting times between steps or when the spatial domain is restricted. $\alpha = 1$ is the standard exponent between the MSD and time, a characteristic of a *diffusive* regime. For $1 < \alpha < 2$, the regime becomes *superdiffusive* and can be encountered in situations where the length of the steps in a random walk is drawn from a distribution with infinite variance, as in the Lévy Walk. Finally, if $\alpha = 2$, the regime is said *ballistic* and the MSD increases quadratically with time.

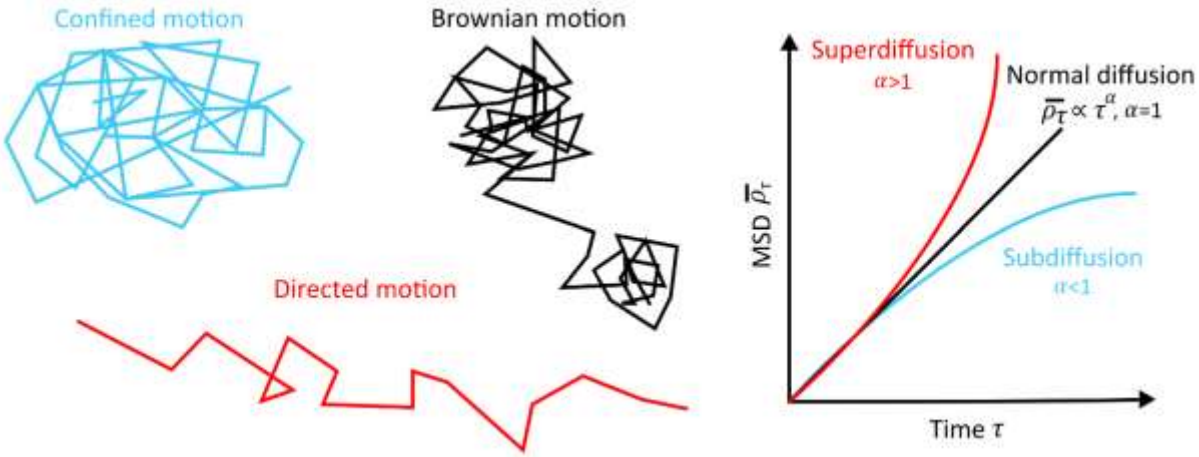

Fig. 2 – Different types of diffusion will result in different trajectories (left), leading to different mean squared displacement (MSD) dependencies as a function of time (right).

Model building

In CoFee-L, the movement of a group of particles exploring their environment in search of food is considered as a perpetual succession of three phases. The first phase, called *cohesion phase*, allows each particle either to move away from neighbouring particles that are too close (rule 1), or to retrace its steps if it has moved too far from the CM of the group (rule 2). Rule 1 is the overriding rule and only one of the two rules can be performed during this first phase. So if a particle A is too far away from the group's CM, but a particle B is within its comfort zone, the particle A will perform an avoidance manoeuvre first (and only). If neither of the two rules apply, the evaluated particle does not move. The second phase, called *exploration phase*, will allow all the particles to perform a random movement in order to explore their surroundings. The applied motion will be a simple random walk, meaning that the direction of the movements will be completely random. Finally, the third and last phase, called *leadership phase*, will allow the group to have a directed movement when the particles have detected FAs in their environ. More precisely, during this phase, each particle will have the opportunity to check if food is present in the surroundings. When a particle detects a source of food, it then becomes a potential leader (if other particles detect other resources, these particles also become potential leaders). Once all the potential leaders are known, the one that turns out to be closest to its FA acquires the status of global leader of the group, while all the other particles become follower particles, the global leader's only role being to lead the followers to the detected FA. In the particular case where no FA has been located, no particle acquires the status of leader and therefore cannot lead the group. In order not to leave the particles inactive and to increase their chances of finding a feeding site, a simple random walk is still applied as in the previous phase. Once the third phase is over, the first phase is started again and so on. At the beginning of each simulation, the group of particles is generated around a FA, as the troop sleeps near FA [31], and the updates of the particle positions are performed in random sequence. An illustration of CoFee-L can be found in the supplementary information (Video *S1*).

Coding and parameters

CoFee-L, coded in the C++ programming language, has been developed on a network in order to reproduce as intuitively as possible the application of the three phases described above to a group of particles. The simulation environment is thus composed of cells that can either be occupied by a particle, a food source (FA>0) or be empty. The basic rule is that two particles cannot be on the same cell, i.e. in the same place, and that only particles are allowed to move on the network. CoFee-L is governed by ten key parameters. ***nbrWalker*** corresponds to the number of particles simulated. ***sizeMap*** is the size (in terms of cells[1]) of an edge of the network. A cell has an area of 1m² and from a practical point of view, the simulations were carried out only on square networks. ***iterations*** is the number of times the 3 phases will be performed during a simulation. The larger the *iterations*, the more the group's position will be updated and the greater the distance covered by the CM. ***precisionCM*** corresponds to the distance (in meters) at which the group's CM is considered to have reached a cell with a food source. For example, *precisionCM* = 10 will mean that as soon as the group's CM is less than 10 meters from a FA, this source will be considered as reached. A destructive encounter dynamic is applied as in a previous study [37], i.e. FAI is set to 0 in order to allow the particles to detect and move towards another FA. The notion of FA deactivation combines two biological realities, namely satiety and resource depletion. ***comfortZone*** intervenes in the priority rule of the first phase of CoFee-L and corresponds (in terms of cells) to the comfort zone of each particle. For example, *comfortZone* = 2 will mean that each particle requires a zone free of any other particle of two cells around it (including diagonals). ***radiusTroop*** also intervenes in the first phase but at the level of the secondary rule and allows to define the radius (in meters) around the CM of the group beyond which a particle will have to return to the CM. This parameter allows the group not to scatter beyond a certain distance and *radiusTroop* = 100 will mean for example that particles can move up to 100m away from the group's CM. ***explorationZone*** intervenes in the second phase and defines (in terms of cells) the exploration

[1] Since the model simulates particles on a grid, it is appropriate to express some parameters in terms of the grid cell.

distance. For example, *explorationZone* = 2 will mean that each particle can move two squares around it (including the diagonals). The larger this parameter is, the further the particles will be able to explore during the exploration phase. ***abundanceReach*** comes into play in the third phase and allows to define (in meters) the range of each FA. The range of a FA is the distance over which it can be detected by a particle. It is defined in CoFee-L as the product of its abundance and *abundanceReach*. As mentioned earlier, the abundance was computed for each FA as the mean P_{sm} for all fruiting trees occupying the FA. Two cases can be distinguished: *abundanceReach* = ∞ and *abundanceReach* > 0. In the first case, all FA have infinite range regardless of their abundance and each particle therefore knows the position of all resources. In the second case, the range of each source depends on the value of *abundanceReach*. Thus, if *abundanceReach* = 100, all sources with an abundance of 4 will be detectable within a radius of 4 × 100 = 400m around them, all sources with an abundance of 1.5 will be detectable within a radius of 1.5 × 100 = 150m, etc (Fig. *3*). This parameter can therefore be seen as the memory of the particles, because the larger it is, the more the particles will know the location of a large number of resources, and vice versa. *abundanceReach* also combines two biological realities, namely the individual's memory of the environment and the remote perception of resources [38, 39]. These two realities form the personal information of an individual. Another parameter comes into play in the third phase, called ***velocity***, the purpose of which is to control the velocity of each particle when a FA is attainable. If *velocity* = 2, the particles will move by a step of 2m at each execution of the third phase. Finally, the last parameter, ***levyRatio***, will prevent the group from remaining confined. For certain values of parameters such as *explorationZone* = 1 and *abundanceReach* = 1, it is possible that the group remains stuck at a place and cannot evolve any more on the map (since particles cannot explore over a long-distance during phase 2 and FA are not very detectable). If *levyRatio* = 5 for example, the parameter *abundanceReach* will change to ∞ after 2000/5 = 400 meters if any FA have been deactivated during this move. For *levyRatio*=25, the group will therefore know the position of every FA on the map if no FA has been deactivated after 2000/25 = 80 meters. The numerator was chosen at 2000m because it is in the range of the daily average distance travelled by the observed troop.

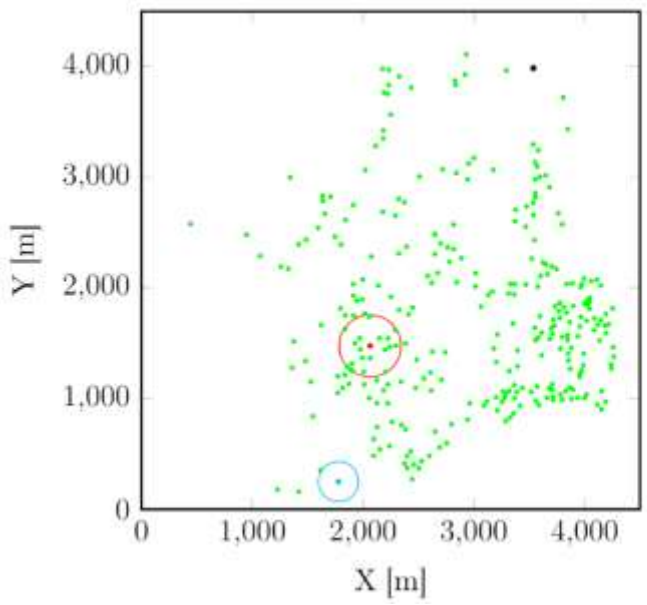

Fig. 3 – Map corresponding to the month of high abundance in the dry evergreen forest. Each green dot points a food source (FA > 0). The circles correspond to the detection range of 3 food sources for abundanceReach = 100 with different values of abundance (red: 2.8, cyan: 1.81, black: 0.27).

In order not to get bogged down with the large number of modifiable parameters, it is necessary to predetermined as many parameters as possible. In particular, *nbrWalker* and *sizeMap* can be set to the number of macaques in the troop (140 individuals) and the size of the different FA maps (4500x4500m²). Then *precisionCM* was fixed to one meter, allowing the group to cluster sufficiently around a FA before moving on to another one. The parameter delimiting the personal space of each particle (*comfortZone*) was set to 1, which represents an area that is neither too large nor too small in relation to the surface area allocated to an individual (1m²). *radiusTroop* was also fixed and set it to *nbrWalker* as it was observed during the field weeks that the troop could sometimes extend up to 300m. Finally, we fixed *iterations* because it is wiser to fix this parameter in order to have comparable results between them. Furthermore, by setting the number of iterations of the simulations rather than the distance travelled by the group, it randomises the total length of the daily trajectories which is more plausible than having fixed daily distances. Thus, from one simulation to another, the group of

particles will be generated at different locations on the map and will therefore have a fixed number of iterations in order to cover a greater or lesser distance depending on the FAs encountered on its path. Under different conditions tested, simulated particles need an average of 19,300 iterations to travel approximately 2,000 meters. With such a value of *iterations*, the position of the group is thus updated approximately every 2 seconds since one day of tracking is equivalent to approximately 43,200sec (12 hours), which is realistic. The control parameters, *abundanceReach, explorationZone, velocity and levyRatio*, were varied to validate the model and to reveal their impact on the movements and the group's foraging dynamics.

Model validation

First, we analysed the field data via an MSD study to establish the type of movement of the macaque troop we are dealing with. Second, we checked how CoFee-L reacted to extreme conditions, following Carson (2002) in order to confirm the basic functioning. Then, to get a better comprehension of the CoFee-L, we analysed and described the simulated trajectories for a set of values of the control parameters. Finally, to compare CoFee-L to the field data, we characterised the simulated trajectories with histograms and χ^2 for step length and turning angle distributions sampled at the same frequency as the collection of field observations.

RESULTS

Field data

During high food availability in the dry evergreen forest, the troop performs a directed movement (i.e. $\bar{\rho}_\tau \propto \tau^\alpha$ with $\alpha > 1$, Fig. *4*) with the mean α = 1.46 +- 0.08. The same kind of trajectories are also found for high (resp. low – N.B. resp. for respectively) food availability in plantations (resp. dry evergreen forest and plantations) with mean α = 1.69 +- 0.08 (resp. α = 1.36 +- 0.15, see Fig. *5, S1 and S2*).

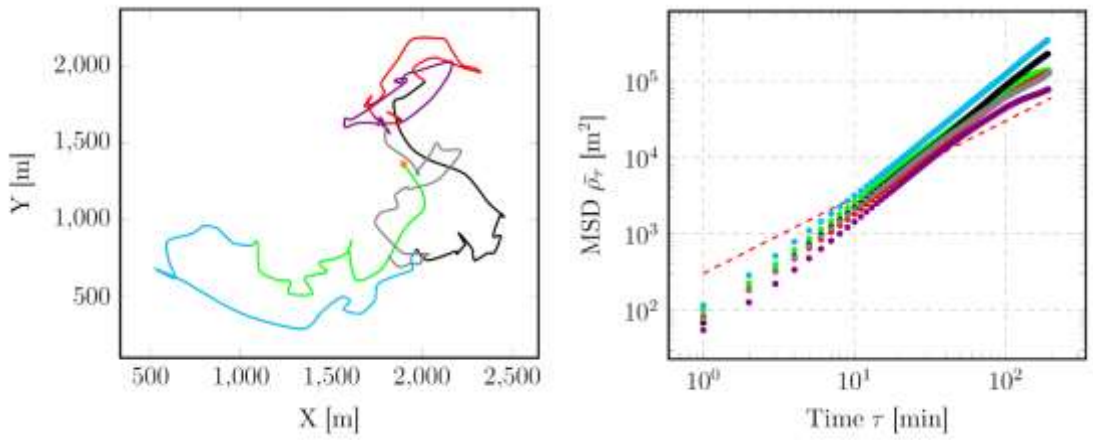

Fig. 4 – Evolution of the troop position (left), with the corresponding mean squared displacements (MSDs, right, mean α = 1.46 +- 0.08) for a tracking of 6 consecutive days during high food availability in the dry evergreen forest. The orange square indicates the departure of the troop and the dashed line represents a line of a unitary slope, i.e. for α = 1.

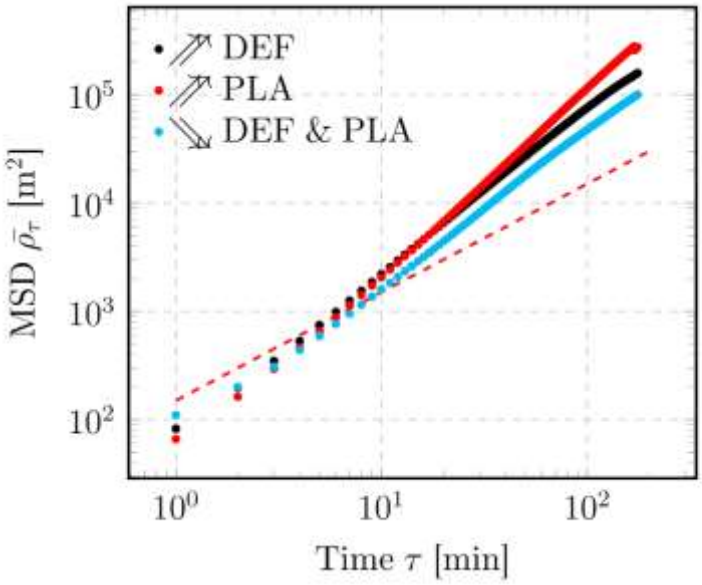

334

335 *Fig. 5 – Average mean squared displacements (MSDs) values of the troop for the three periods of fruit abundance*
336 *(DEF for dry evergreen forest and PLA for plantations). The dashed line represents a line of a unitary slope, i.e. for*
337 *α = 1.*

338

339 For all other observation periods, the mean exponent *α* varies in relatively the same range
340 independently of the abundance of fruits in the study site (Fig. *6*).

341

342

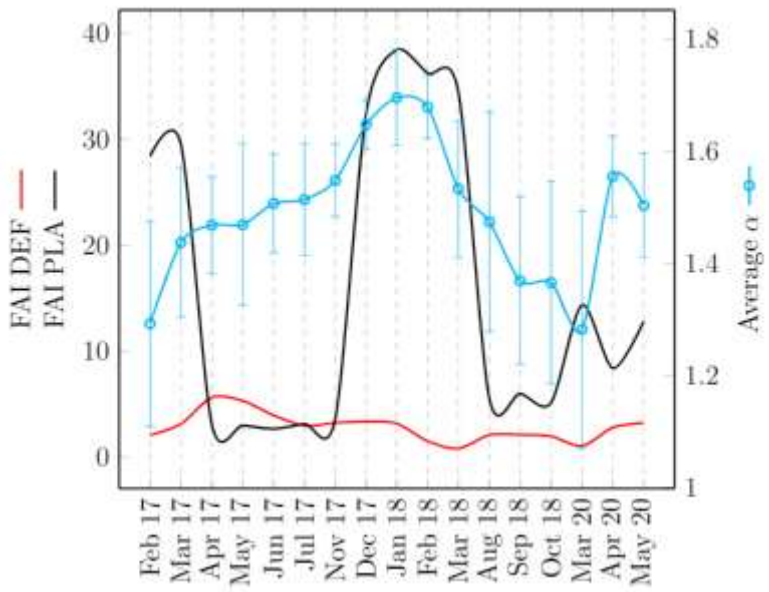

Fig. 6 – Food availability index (FAI) and average α as a function of the different periods of monitoring of the troop. The red (resp. black) curve represents the FAI for the dry evergreen forest (DEF) (resp. plantations, PLA) and is plotted along the left-hand y-axis. The cyan curve represents the variation of the average α and is plotted along the right-hand y-axis.

CoFee-L flexibility analysis

A diffusive regime is obtained if the particles are generated in a location free of FAs with the control parameters *abundanceReach* = 0.1 and *explorationZone* = 1[2]. These conditions establish extremely small range for each FA and the particles are only able to explore the map over short distances. Secondly, a ballistic regime, is obtained when the group of particles is generated in an area where FAs are present with the control parameters *abundanceReach* = ∞ and *explorationZone* = 2. In this latter case, in addition to being able to explore the map over larger distances, each particle knows the location as well as the abundance of all FAs (Fig. *7*).

[2] For this section, the control parameters *velocity* = *levyRatio* = 1 in order to facilitate the understanding and interpretation of the different basic behaviours of the model.

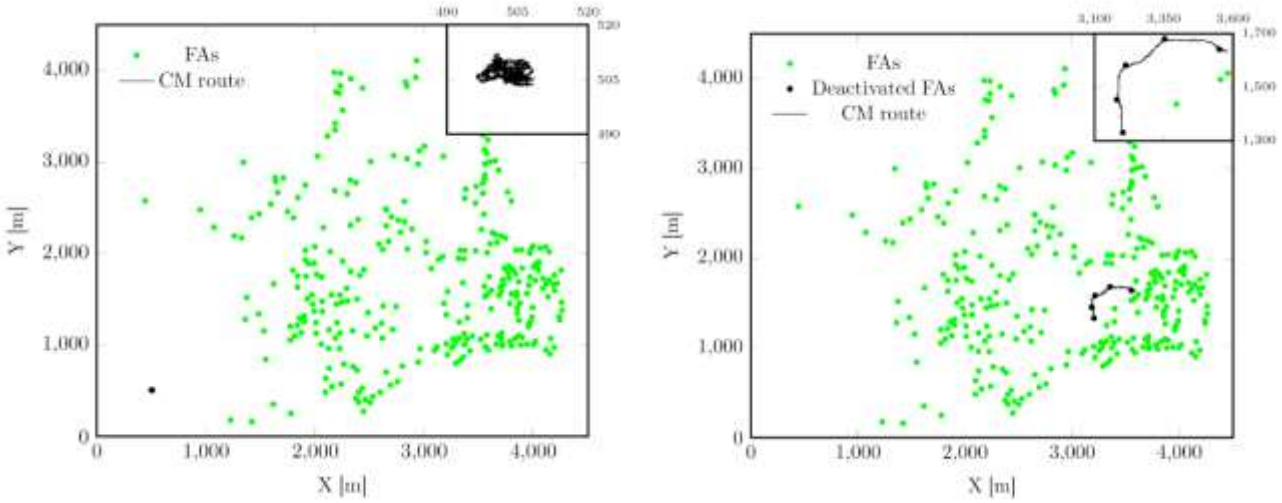

357

358 *Fig. 7 – Centre of mass (CM) trajectories on a map of high food availability in the dry evergreen forest with control*
359 *parameters abundanceReach = 1, explorationZone = 1 (left) and abundanceReach = ∞, explorationZone = 2*
360 *(right). In both cases, velocity = levyRatio = 1. Deactivated feeding areas (FAs) are those through which the group's*
361 *CM has passed within precisionCM metres. A magnification of the CM trajectory is shown in the upper right*
362 *corner.*

363

364 When *explorationZone* is kept fixed, it can be observed that for *abundanceReach* = ∞, the group
365 efficiently crosses the map in all cases (Fig. *8*). In contrast, if the memory is small (*abundanceReach* =
366 5), the group get stuck around its generation location because the particles have to randomly explore
367 their environment for a period longer than 19,300 iterations in order to hope to enter the range of a
368 FA. For an intermediate value (*abundanceReach* = 50), the group can either be blocked or take
369 advantage of the FAs in its surroundings, depending on where it is initially generated. One can also
370 notice that the CM does not follow the same trajectory depending of the value of *abundanceReach*.
371 Since the particles can extend up to 140m around the CM and the second phase of CoFee-L allows for
372 randomisation of the motion, different trajectories can be chosen throughout each simulation.

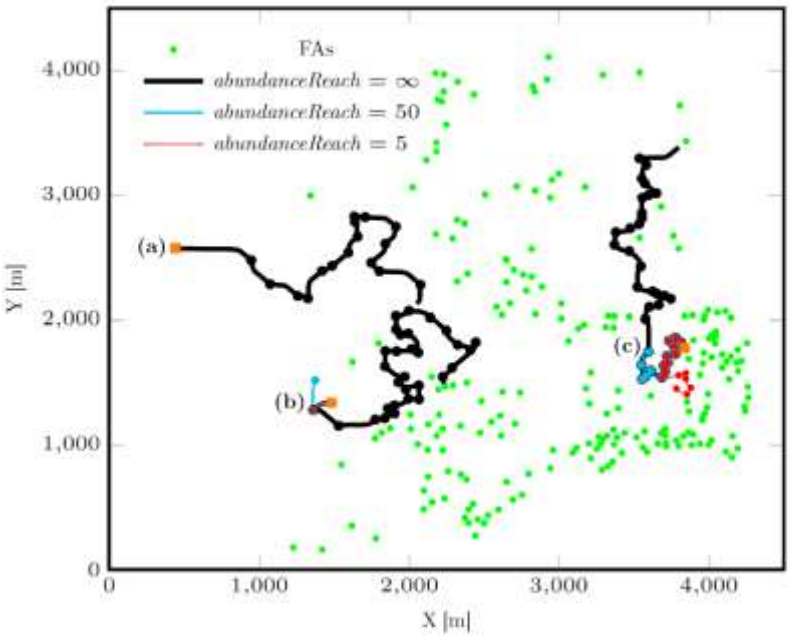

373

374 *Fig. 8 – Centre of mass (CM) trajectories for explorationZone = 1 and abundanceReach values of 5, 50 and ∞. The*
375 *orange square indicates where the group of particles was generated. In (a) and (b), the CM remains stuck for*
376 *abundanceReach = 5 and 50. In (c), due to a higher density of feeding area (FA), each value of abundanceReach*
377 *allows the CM of the group to progress.*

378

379 Keeping *abundanceReach* fixed, we observed longer trajectories and more deactivated FAs for higher
380 values of *explorationZone,* except in places too remote with low density of FA (Fig. *9*).

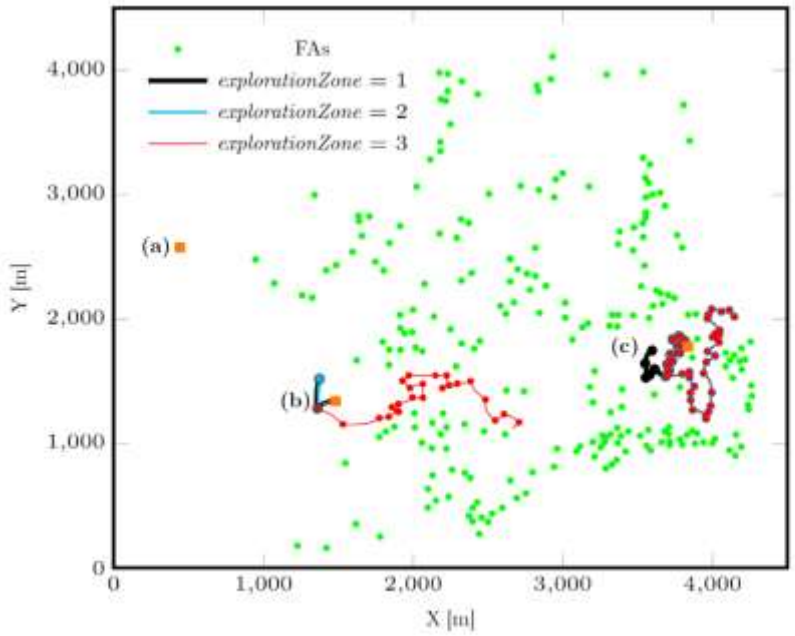

Fig. 9 – Centre of mass (CM) trajectories for abundanceReach = 50 and explorationZone values of 1, 2 and 3. The orange square indicates where the group of particles was generated. In (a), the group remain completely stuck at the initial generation point. In (b), the particles progress only for explorationZone = 3. In (c), the density of feeding area (FA) is much higher and the particles can therefore go in many different directions as soon as the value of the exploration parameter is varied.

CoFee-L calibration

Tuning only with control parameters *abundanceReach* and *explorationZone* is not enough to have realistic trajectories of simulated particles. Although χ^2 to compare step length and turning angle distributions between observed and simulated trajectories are generally satisfying for *explorationZone* = 2 and *abundanceReach* comprised between 5 and 50, trajectories are too short compared to data field (Fig. *10*, *S3* and *S4*).

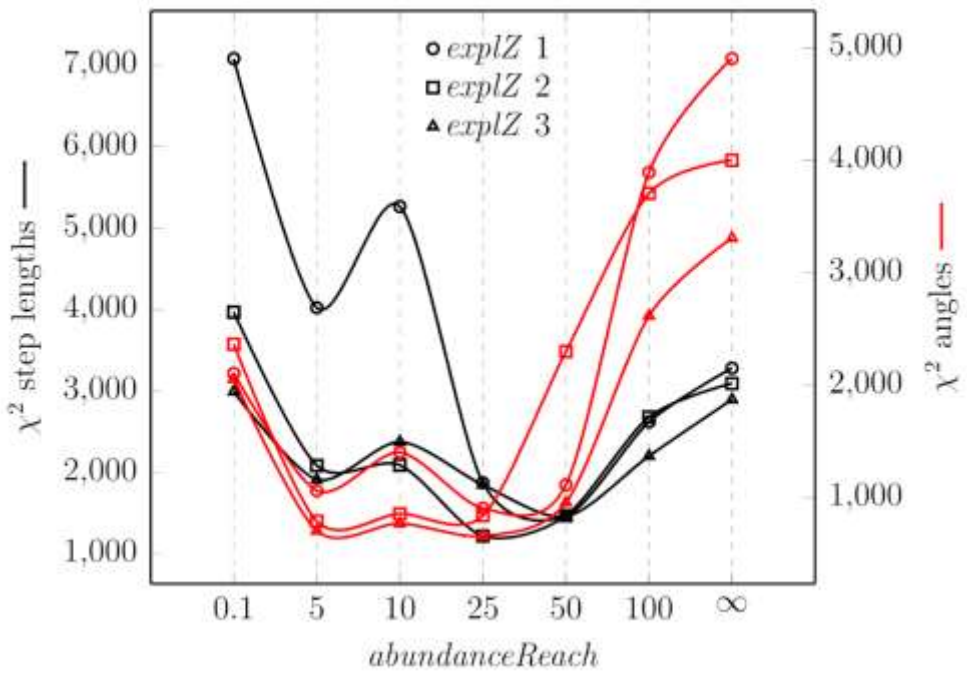

394

395 *Fig. 10 – χ^2 for comparing step length and angle distributions between observed and simulated trajectories as a*
396 *function of abundanceReach, for velocity = levyRatio = 1 and explorationZone = 1, 2 and 3. The black (resp. red)*
397 *curves represent the χ^2 for step lengths (resp. angles) and are plotted along the left-hand (resp. right-hand) y-*
398 *axis. For each simulation, the group of particles was simulated from the same starting point and on a map of high*
399 *food availability in the dry evergreen forest.*

400

401 To increase the realism, we have to tune the control parameter *levyRatio* since large-scale animal
402 movements turn out to be a successive combination of clusters of steps separated by long trips [37].
403 A satisfying χ^2 is obtained from approximately *levyRatio* = 35, independently of the abundance of fruits,
404 when *abundanceReach* = 0.1 and *explorationZone* = 2 (Fig. *11*). In this way, the group of simulated
405 particles can perform a random movement (given that *abundanceReach* is very small) up to a certain
406 distance (determined by *levyRatio*) after which *abundanceReach* turn to ∞, so the group can perform
407 a directed movement.

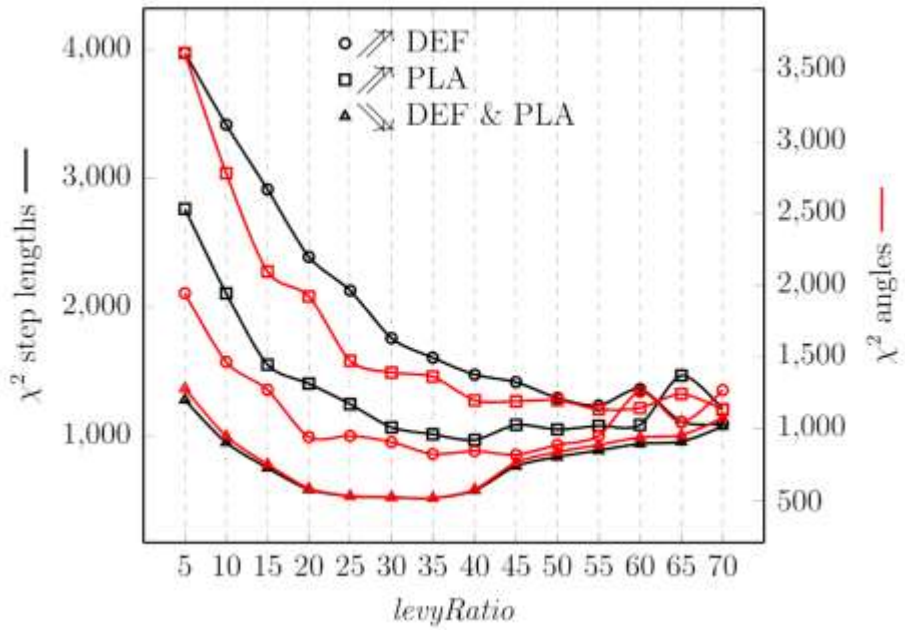

408

409 *Fig. 11 – χ^2 for comparing step length and angle distributions between observed and simulated trajectories as a*
410 *function of levyRatio, with control parameters abundanceReach = 0.1, explorationZone = 2 and velocity = 1. The*
411 *black (resp. red) curves represent the χ^2 for step lengths (resp. angles) and are plotted along the left-hand (resp.*
412 *right-hand) y-axis. For each period of food abundance (DEF for dry evergreen forest and PLA for plantations), the*
413 *group of particles was simulated from the same starting point at three random positions.*

414

415 For example, a similar trajectory to the field data for the period of high food abundance in the dry
416 evergreen forest can be observed when *levyRatio* = 35, both from a χ^2, histogram and MSD perspective
417 (Fig. *12* and *13*). During high food abundance in plantations (resp. low food abundance in the dry
418 evergreen forest and plantations), it is *levyRatio* = 60 (resp. also *levyRatio* = 35) which does a better
419 job (Fig. *S5-8*).

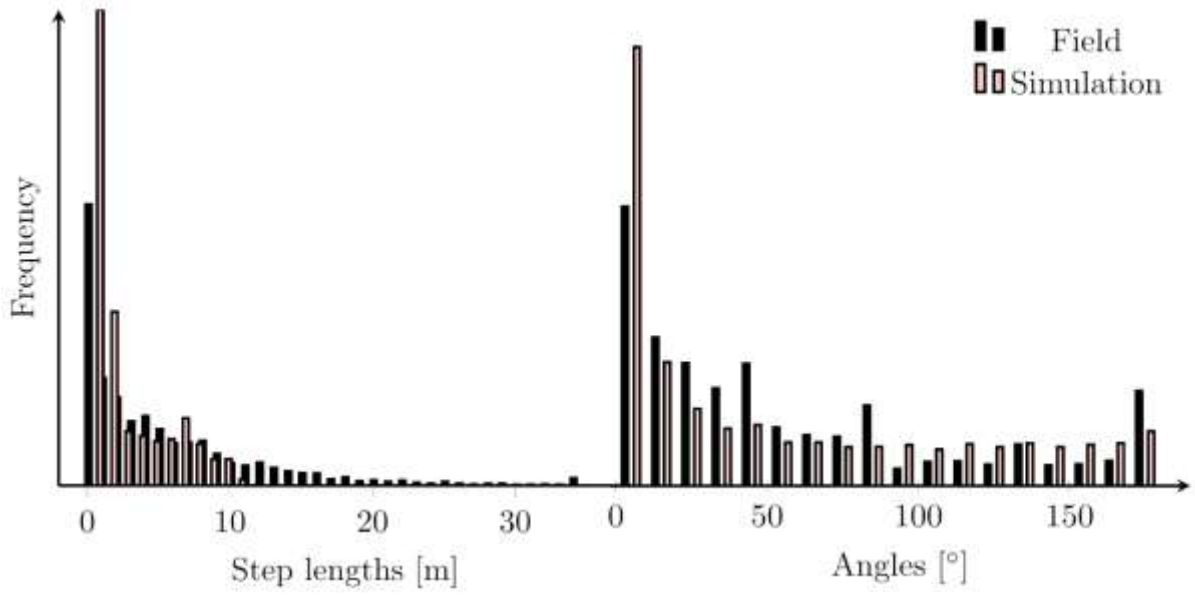

420

421 *Fig. 12 – Histogram of step lengths (left) and angles (right) for field (black) and simulation (red) data during high*
422 *food availability in the dry evergreen forest, with control parameters abundanceReach = 0.1, explorationZone =*
423 *2, velocity = 1 and levyRatio = 35.* χ^2 *= 1517 (resp. 942) for step lengths (resp. angles).*

424

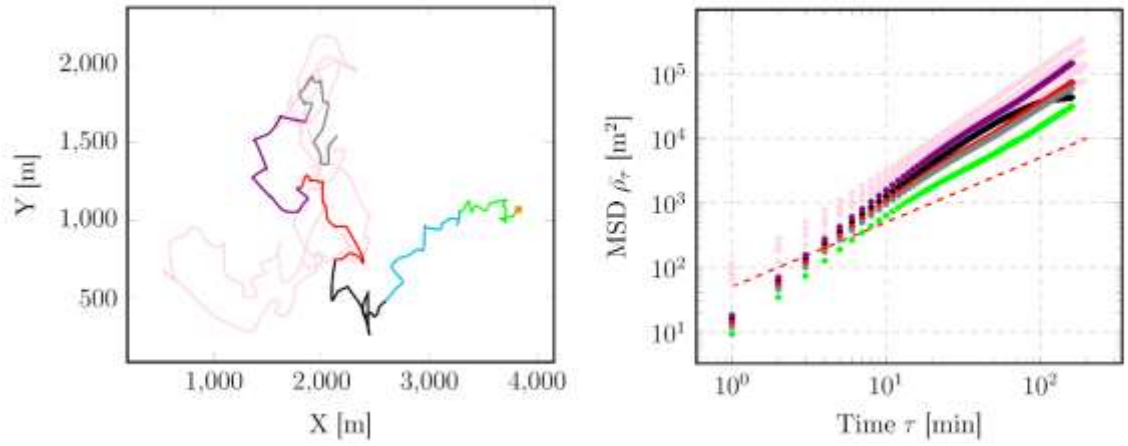

425

426 *Fig. 13 – Evolution of the group position (left), with the corresponding mean squared displacements (MSDs, right,*
427 *mean α = 1.53 +- 0.08) for a simulation of 6 consecutive days during high food availability in the dry evergreen*
428 *forest, with control parameters abundanceReach = 0.1, explorationZone = 2, velocity = 1 and levyRatio = 35. Pink*
429 *trajectories and MSDs represent the troop data. The orange square indicates the departure of the group of*
430 *particles and the dashed line represents a line of a unitary slope, i.e. for α = 1.*

Variation of control parameter *velocity* does not improve the quality of simulations, regardless of the period of abundance (Fig. *14*).

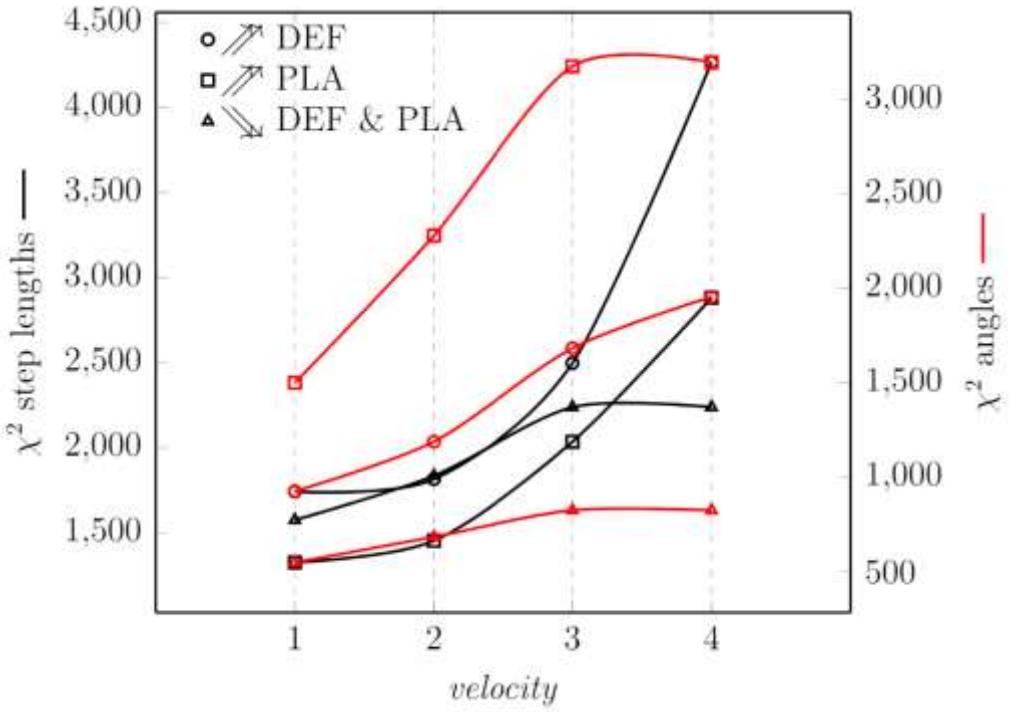

Fig. 14 – χ^2 for comparing step length and angle distributions between observed and simulated trajectories as a function of velocity, with control parameters abundanceReach = 0.1, explorationZone = 2 and levyRatio = 25. The black (resp. red) curves represent the χ^2 for step length (resp. angles) and are plotted along the left-hand (resp. right-hand) y-axis. For each period of food abundance (DEF for dry evergreen forest and PLA for plantations), the group of particles was simulated from the same starting point.

DISCUSSION

In general, animal movement models explain only one aspect of the behaviour, such as the coherence of the community, the daily variation of movements or the importance of the distribution of food resources [9, 12, 15-19, 26, 27]. CoFee-L combines these different aspects, regardless of the size of the group studied, and simulates the individual movement of each group member, which is important to consider when groups of animals have many individuals that move apart from each other. It allows us to reproduce the physical properties of the troop's CM trajectory (MSDs), as well as the step length and angle distributions of the field data. Moreover, the parameterisation is rather simple, since it is only necessary to fix a set of parameters easily observable in the field (here: *nbrWalker* = 140, *sizeMap* = 4500*, precisionCM* = 1*, comfortZone* = 1*, radiusTroop* = 140 and *iterations* = 19,300), and then to adjust the values of 4 parameters which have biological meaning (here: *AbundanceReach* = 0.1, *explorationZone* = 2, *velocity* = 1 and *levyRatio* = 35 or 60 depending on the season of observation).

Correlated random walks and levy walks are considered the most optimal strategies in the random search problem [40]. In CoFee-L, if we need to simulate organisms performing trajectories similar to those of the levy walk, it is sufficient to set *abundanceReach* to 0.1 and *explorationZone* to 2, find the right *velocity* according to the species studied and look for the right *levyRatio* parameter that minimises the χ^2 comparing the observed and simulated distributions of angles and segments. In cases where the studied individuals are performing a movement corresponding rather to a correlated random walk, the *levyRatio* parameter can be deactivated and it is then sufficient to look for the right values of the other three control parameters. In the case of the macaque troop in Sakaerat, they were apparently performing levy walks, like many other primates [39, 41-44].

The troop in Sakaerat uses four feeding strategies depending on the seasonality of the resources [1, 29-31]. Macaques rely on a "high-cost, high-yield[3]" strategy during the period of high abundance in plantations by increasing their daily trajectories and home range. During the period of high abundance in the dry evergreen forest, the troop rather displays a "low-cost, high-yield" strategy by intensively foraging in the centre of their home range. And during the period of low abundance in dry evergreen forest and plantations, the troop combines the latter two strategies. In the simulations, the control parameter *levyRatio* must therefore be used to differentiate between the different periods of food abundance in the movements of the particles in the group. The more it increases, the less the group will be stuck in a place without FAs.

Later, in order to increase the realism of the simulations, several concepts of CoFee-L could be improved. First of all, the third phase of the model could be reconsidered. On one hand, the extent of leadership in relation to followers is not representative of what happens in large groups of wild animals because the followers furthest away from the leader perceive his dominance in the same way as those who are closest. On the other hand, each individual in the group has the same weight in the decision-making process. However, there are about 80 juveniles and infants among the 140 individuals considered who almost never take the initiative on the location of a resource [45]. The *leadership phase* of CoFee-L must therefore be adjusted to increase biological realism. Secondly, CoFee-L does not take into account the fission-fusion phenomenon (as shown in Video *S2*). In the case of macaques and other species that form large groups, individuals split into several subgroups for feeding (and thus use several FAs at the same time) and join each other during large movements [46, 47]. Then, departure and/or arrival generation points could be set up, as some species have particular sleeping sites (e.g. [32, 48, 49]). In the current context, given the degradation of the environment and low fruit

[3] High-cost (resp. low-cost) means that individuals make high (resp. low) efforts and thus high (resp. low) energy costs when searching for food. This is characterised for example by an increase (resp. decrease) in the length of daily trips. High-yield (resp. low-yield) means that individuals benefit from a high (resp. low) energy input during foraging due to high (resp. low) nutrient quality and high (resp. low) abundance of native, exotic and/or human resources.

availability, the group was simulated and ended its days around FAs to presumably maximize energy intake which was observed in the field [31] and in other species like the bonobo [50]. The edge effect could also be taken into account in the future in order to simulate animal communities evolving in a continuous environment. It is important to develop an approach to limit simulation zones by animal species, and thus to spatially limit the action of an animal species on the dispersal of a plant species, using the data on home range sizes for example. Finally, it could also be interesting to consider rest periods for the different possibilities of action of the group of particles.

Despite the lack of individual data, CoFee-L is able to realistically reproduce the movement of the CM of the troop. It can therefore be generalised to other types of animals, which is perfectly in line with our future objective of calculating the seed rain they generate. The concept of total seed dispersal kernels (TDK), i.e. the overall probability of dispersion of a plant individual, population, species or community, combining influence of all primary, secondary and higher-order dispersal vectors has been reviewed, but few studies have tried to obtain TDK for given species. While approaches based on seed rain sampling combined with statistical approaches appear challenging, on the contrary, the identification of fruit-frugivores networks and the most contributing vectors has recently experienced great strides [51]. In this framework, mechanistic modelling, including animal movements, their interactions with the fruiting trees and their physiological requirements becomes easier to consider and this kind of methodology looks able to exploit the available datasets. For instance, the model MOST was built and validated for the seed deposition of the genus *Pourouma* produced by a small group of 4 Golden-headed lion tamarins (*Leontopithecus chrysomelas*) [48]. The animal trajectories in their seasonal home range were analysed with hidden Markov modelling which further allows generating state transitions related to local environmental characteristics and accordingly, random steps and turning angles. However, such a model for movement is only appropriate for animal species

514 living in small clusters. It could be upgrade thanks to CoFee-L to simulate TDK for given tree species
515 resulting from the activity of the ad hoc set of animal species living in large groups or not.

516

517 CONCLUSIONS

518 We developed the CoFee-L model to simulate the individual movements of animals living in large
519 groups. It is quite easy to parametrize with elementary observable information in the field and with 4
520 parameters characterizing the behaviour of the species. The distribution and the food abundance
521 govern the individual movements in the home range. The model could be refined by improving the
522 leadership assignment or adding constrains concerning for instance the reuse of sleeping sites.

523

524 Using CoFee-L, we planned to improve a model of zoochoric seed dispersal to obtain the combined
525 effect of the main dispersing agents and the TDK of a given tree species. Ultimately, we could predict
526 the shift and the turnover of zoochoric tropical trees species with a dynamic vegetation model (DVM,
527 e.g. [7, 52]), under future climate hypotheses. A DVM is able to compute gross photosynthesis and
528 respiration and to allocate fixed carbon to the short-lived and the perennial parts of the plants it
529 simulates, from input data such as monthly climate and atmospheric CO_2 concentration and traits
530 describing the plant species, such as the specific leaf area and the nitrogen concentration. The DVMs
531 realize transient simulations, i.e. running over time, at several thousands of places. Yet, DVMs produce
532 only suitability and potential growth for the selected species. Then by dispersing seeds in the area of
533 interest (for instance with CoFee-L), we could record the annual fate of each seed in terms of
534 germination success or failure, followed by growth, development or dead over several decades.
535 However, as the TDK depends also on animal density which itself is influenced by hunting [53-55] but
536 also by the loss of surfaces devoted to forests [56], it appears impossible to simulate existing situations.

Therefore, the modelling will allow to test a variety of conditions of landscape continuity and animal densities in the framework of climate change.

LIST OF ABBREVIATIONS

DEF – Dry Evergreen Forest;

PLA – PLAntations;

CM – Centre of Mass;

FA – Feeding Area;

FAI – Food Availability Index;

MSD – Mean Squared Displacement;

TDK – Total seed Dispersal Kernels;

DVM – Dynamic Vegetation Model.

DECLARATIONS

ETHICAL APPROVAL AND CONSENT TO PARTICIPATE

The monitoring work was conducted under the authorisation of the National Research Council of Thailand.

CONSENT FOR PUBLICATION

Not applicable.

AVAILABILITY OF SUPPORTING DATA

The datasets used and analysed during the current study are available from the corresponding author on reasonable request.

COMPETING INTERESTS

The authors declare that they have no competing interests.

FUNDING

This work was supported by PACODEL and SSE of the University of Liege for the field work in Thailand, and by the Unit of Research SPHERES for the writing of the article.

AUTHORS' CONTRIBUTIONS

EG and NG conducted the field work. NG, NW and AH contributed to the design of CoFee-L. JD critically reviewed drafts. NG and AH wrote the manuscript. The authors read and approved the final manuscript.

ACKNOWLEDGEMENTS

We would like to thank Fany Brotcorne who helped us organise the field campaign in Thailand. Thanks also to the people from PACODEL and SSE of the University of Liège who followed and supported us during the SARS-CoV-2 crisis. Finally, thanks to all the Sakaerat staff for their welcome and kindness.

AUTHORS' INFORMATION

Not applicable

REFERENCES

1. Gazagne E, José-Domínguez JM, Huynen MC, Hambuckers A, Poncin P, Savini T, et al. Northern pigtailed macaques rely on old growth plantations to offset low fruit availability in a degraded forest fragment. American journal of primatology. 2020;82(5):e23117.

2. Morante-Filho JC, Arroyo-Rodríguez V, Pessoa MdS, Cazetta E, Faria D. Direct and cascading effects of landscape structure on tropical forest and non-forest frugivorous birds. Ecological applications. 2018;28(8):2024-32.

3. Mangan SA, Schnitzer SA, Herre EA, Mack KM, Valencia MC, Sanchez EI, et al. Negative plant–soil feedback predicts tree-species relative abundance in a tropical forest. Nature. 2010;466(7307):752-5.

4. Fadrique B, Báez S, Duque Á, Malizia A, Blundo C, Carilla J, et al. Widespread but heterogeneous responses of Andean forests to climate change. Nature. 2018;564(7735):207-12.

5. Steinbauer MJ, Grytnes J-A, Jurasinski G, Kulonen A, Lenoir J, Pauli H, et al. Accelerated increase in plant species richness on mountain summits is linked to warming. Nature. 2018;556(7700):231-4.

6. Boisvert-Marsh L, Périé C, de Blois S. Shifting with climate? Evidence for recent changes in tree species distribution at high latitudes. Ecosphere. 2014;5(7):1-33.

7. François L, Hambuckers A. Modeling past plant species' distributions in mountainous areas: A way to improve our knowledge of future climate change impacts? Past Global Changes Magazine. 2020;28(1):16-7.

8. Vicsek T. Fluctuations and scaling in biology: Oxford University Press New York; 2001.

9. Couzin ID, Krause J, James R, Ruxton GD, Franks NR. Collective memory and spatial sorting in animal groups. Journal of theoretical biology. 2002;218(1):1-11.

10. Vicsek T, Zafeiris A. Collective motion. Physics reports. 2012;517(3-4):71-140.

601 11. O'brien D. Analysis of the internal arrangement of individuals within crustacean aggregations
602 (Euphausiacea, Mysidacea). Journal of Experimental Marine Biology and Ecology. 1989;128(1):1-30.
603 12. Vicsek T, Czirók A, Ben-Jacob E, Cohen I, Shochet O. Novel type of phase transition in a
604 system of self-driven particles. Physical review letters. 1995;75(6):1226.
605 13. Partridge BL, Pitcher TJ. The sensory basis of fish schools: relative roles of lateral line and
606 vision. Journal of comparative physiology. 1980;135(4):315-25.
607 14. Krause J, Ruxton GD, Ruxton G, Ruxton IG. Living in groups: Oxford University Press; 2002.
608 15. Aoki I. A simulation study on the schooling mechanism in fish. Bulletin of the Japan Society of
609 Scientific Fisheries. 1982;48(8):1081-8.
610 16. Heppner F. A stochastic nonlinear model for coordinated bird flocks. The ubiquity of chaos.
611 1990.
612 17. Inada Y, Kawachi K. Order and flexibility in the motion of fish schools. Journal of theoretical
613 Biology. 2002;214(3):371-87.
614 18. Kunz H, Hemelrijk CK. Artificial fish schools: collective effects of school size, body size, and
615 body form. Artificial life. 2003;9(3):237-53.
616 19. Kolpas A, Busch M, Li H, Couzin ID, Petzold L, Moehlis J. How the spatial position of
617 individuals affects their influence on swarms: a numerical comparison of two popular swarm
618 dynamics models. PloS one. 2013;8(3):e58525.
619 20. Couzin ID, Krause J, Franks NR, Levin SA. Effective leadership and decision-making in animal
620 groups on the move. Nature. 2005;433(7025):513-6.
621 21. Miller N, Garnier S, Hartnett AT, Couzin ID. Both information and social cohesion determine
622 collective decisions in animal groups. Proceedings of the National Academy of Sciences.
623 2013;110(13):5263-8.
624 22. Sueur C, Petit O. Organization of group members at departure is driven by social structure in
625 Macaca. International Journal of Primatology. 2008;29(4):1085-98.

626 23. Nagy M, Ákos Z, Biro D, Vicsek T. Hierarchical group dynamics in pigeon flocks. Nature.
627 2010;464(7290):890-3.
628 24. Grueter CC, Chapais B, Zinner D. Evolution of multilevel social systems in nonhuman primates
629 and humans. International Journal of Primatology. 2012;33(5):1002-37.
630 25. Jia Y, Vicsek T. Modelling hierarchical flocking. New Journal of Physics. 2019;21(9):093048.
631 26. Ozogány K, Vicsek T. Modeling the emergence of modular leadership hierarchy during the
632 collective motion of herds made of harems. Journal of Statistical Physics. 2015;158(3):628-46.
633 27. Ferdinandy B, Ozogány K, Vicsek T. Collective motion of groups of self-propelled particles
634 following interacting leaders. Physica A: Statistical Mechanics and its Applications. 2017;479:467-77.
635 28. Strandburg-Peshkin A, Farine DR, Couzin ID, Crofoot MC. Shared decision-making drives
636 collective movement in wild baboons. Science. 2015;348(6241):1358-61.
637 29. Gazagne E, Hambuckers A, Savini T, Poncin P, Huynen M-C, Brotcorne F. Toward a better
638 understanding of habituation process to human observer: A statistical approach in Macaca leonina
639 (Primates: Cercopithecidea). Raffles Bulletin of Zoology. 2020;68(2020):735-49.
640 30. Gazagne E, Pitance J-L, Savini T, Huynen M-C, Poncin P, Brotcorne F, et al. Seed shadows of
641 northern pigtailed macaques within a degraded forest fragment, Thailand. Forests.
642 2020;11(11):1184.
643 31. Gazagne E, Savini T, Ngoprasert D, Poncin P, Huynen M-C, Brotcorne F. When northern
644 pigtailed macaques (Macaca leonina) cannot select for ideal sleeping sites in a degraded habitat.
645 International Journal of Primatology. 2020;41(4):614-33.
646 32. Albert A, Hambuckers A, Culot L, Savini T, Huynen M-C. Frugivory and seed dispersal by
647 northern pigtailed macaques (Macaca leonina), in Thailand. International Journal of Primatology.
648 2013;34(1):170-93.
649 33. Wang Y, Jeong Y, Jhiang SM, Yu L, Menq C-H. Quantitative characterization of cell behaviors
650 through cell cycle progression via automated cell tracking. PloS one. 2014;9(6):e98762.

651 34. Saxton MJ. Single-particle tracking: the distribution of diffusion coefficients. Biophysical
652 journal. 1997;72(4):1744-53.
653 35. Havlin S, Ben-Avraham D. Diffusion in disordered media. Advances in physics.
654 1987;36(6):695-798.
655 36. Jeon J-H, Leijnse N, Oddershede LB, Metzler R. Anomalous diffusion and power-law
656 relaxation of the time averaged mean squared displacement in worm-like micellar solutions. New
657 Journal of Physics. 2013;15(4):045011.
658 37. Bartumeus F, da Luz MGE, Viswanathan GM, Catalan J. Animal search strategies: a
659 quantitative random-walk analysis. Ecology. 2005;86(11):3078-87.
660 38. Nabe-Nielsen J, Tougaard J, Teilmann J, Lucke K, Forchhammer MC. How a simple adaptive
661 foraging strategy can lead to emergent home ranges and increased food intake. Oikos.
662 2013;122(9):1307-16.
663 39. Boyer D, Ramos-Fernández G, Miramontes O, Mateos JL, Cocho G, Larralde H, et al. Scale-free
664 foraging by primates emerges from their interaction with a complex environment. Proceedings of the
665 Royal Society B: Biological Sciences. 2006;273(1595):1743-50.
666 40. Raposo E, Buldyrev S, Da Luz M, Viswanathan G, Stanley H. Lévy flights and random searches.
667 Journal of Physics A: mathematical and theoretical. 2009;42(43):434003.
668 41. Reyna-Hurtado R, Teichroeb JA, Bonnell TR, Hernández-Sarabia RU, Vickers SM, Serio-Silva JC,
669 et al. Primates adjust movement strategies due to changing food availability. Behavioral Ecology.
670 2018;29(2):368-76.
671 42. Sueur C, Briard L, Petit O. Individual analyses of Lévy walk in semi-free ranging Tonkean
672 macaques (Macaca tonkeana). PLoS One. 2011;6(10):e26788.
673 43. Raichlen DA, Wood BM, Gordon AD, Mabulla AZ, Marlowe FW, Pontzer H. Evidence of Lévy
674 walk foraging patterns in human hunter–gatherers. Proceedings of the National Academy of
675 Sciences. 2014;111(2):728-33.

676 44. Ramos-Fernández G, Mateos JL, Miramontes O, Cocho G, Larralde H, Ayala-Orozco B. Lévy
677 walk patterns in the foraging movements of spider monkeys (Ateles geoffroyi). Behavioral ecology
678 and Sociobiology. 2004;55(3):223-30.
679 45. Conradt L, Roper TJ. Consensus decision making in animals. Trends in ecology & evolution.
680 2005;20(8):449-56.
681 46. Amici F, Aureli F, Call J. Fission-fusion dynamics, behavioral flexibility, and inhibitory control
682 in primates. Current Biology. 2008;18(18):1415-9.
683 47. Aureli F, Schaffner CM, Boesch C, Bearder SK, Call J, Chapman CA, et al. Fission-fusion
684 dynamics: new research frameworks. Current Anthropology. 2008;49(4):627-54.
685 48. Raghunathan N, François L, Cazetta E, Pitance J-L, De Vleeschouwer K, Hambuckers A.
686 Deterministic modelling of seed dispersal based on observed behaviours of an endemic primate in
687 Brazil. Plos one. 2020;15(12):e0244220.
688 49. José-Domínguez JM, Asensio N, García CJG, Huynen M-C, Savini T. Exploring the multiple
689 functions of sleeping sites in northern pigtailed macaques (Macaca leonina). International Journal of
690 Primatology. 2015;36(5):948-66.
691 50. Serckx A, Huynen M-C, Bastin J-F, Hambuckers A, Beudels-Jamar RC, Vimond M, et al. Nest
692 grouping patterns of bonobos (Pan paniscus) in relation to fruit availability in a forest-savannah
693 mosaic. PloS one. 2014;9(4):e93742.
694 51. Rogers HS, Beckman NG, Hartig F, Johnson JS, Pufal G, Shea K, et al. The total dispersal
695 kernel: a review and future directions. AoB Plants. 2019;11(5):plz042.
696 52. Hambuckers A, Trolliet F, Dury M, Henrot A-J, Porteman K, El Hasnaoui Y, et al. Towards a
697 more realistic simulation of plant species with a dynamic vegetation model using field-measured
698 traits: the Atlas cedar, a case study. Forests. 2022;13(3):446.
699 53. Trolliet F, Forget P-M, Doucet J-L, Gillet J-F, Hambuckers A. Frugivorous birds influence the
700 spatial organization of tropical forests through the generation of seedling recruitment foci under
701 zoochoric trees. Acta Oecologica. 2017;85:69-76.

54. Trolliet F, Forget PM, Huynen MC, Hambuckers A. Forest cover, hunting pressure, and fruit availability influence seed dispersal in a forest-savanna mosaic in the Congo Basin. Biotropica. 2017;49(3):337-45.

55. Boissier O, Feer F, Henry PY, Forget PM. Modifications of the rain forest frugivore community are associated with reduced seed removal at the community level. Ecological Applications. 2020;30(4):e02086.

56. Hambuckers A, Trolliet F, Simon A, Cazetta E, Rocha-Santos L. Seed Removal Rates in Forest Remnants Respond to Forest Loss at the Landscape Scale. Forests. 2020;11(11):1144.

SUPPLEMENTARY INFORMATION

ADDITIONAL FILE 1. Videos showing CoFee-L.

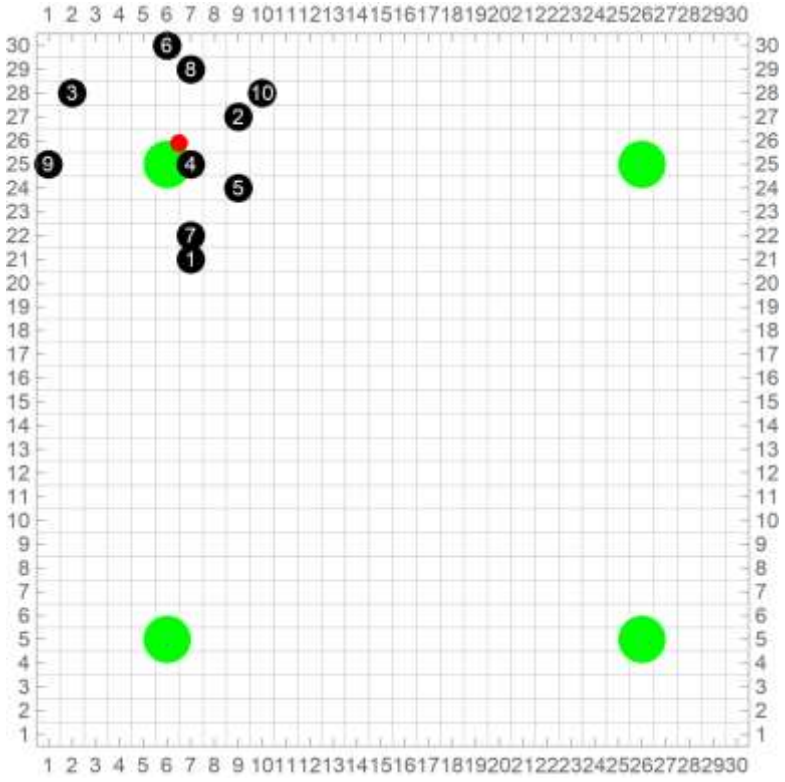

Video S1 – A basic example with 10 particles to illustrate the 3 phases of CoFee-L. The green (resp. red) discs represent the active (resp. inactive) feeding areas, while the small black discs are the simulated individuals. The centre of mass of the group and its displacement pattern are shown in red. The leaders are shown in orange.

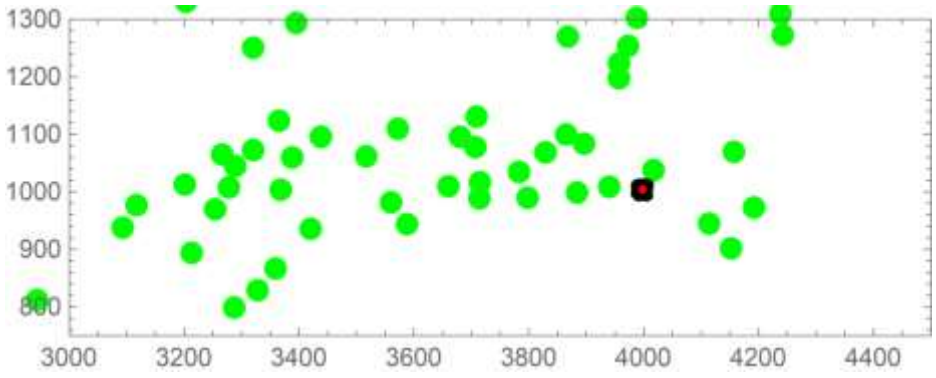

730

731 *Video S2 - Example of a simulation of a day of monitoring, with a zoom on the area of interest in order to visualize*
732 *the 140 particles as well as possible. The green (resp. red) discs represent the active (resp. inactive) feeding areas,*
733 *while the small black discs are the simulated individuals. The centre of mass of the group and its displacement*
734 *pattern are shown in red. The leaders are shown in orange.*

735

736 ADDITIONAL FILE 2. Results concerning the periods of high food availability in plantations & low food
737 availability in dry evergreen forest and plantations.

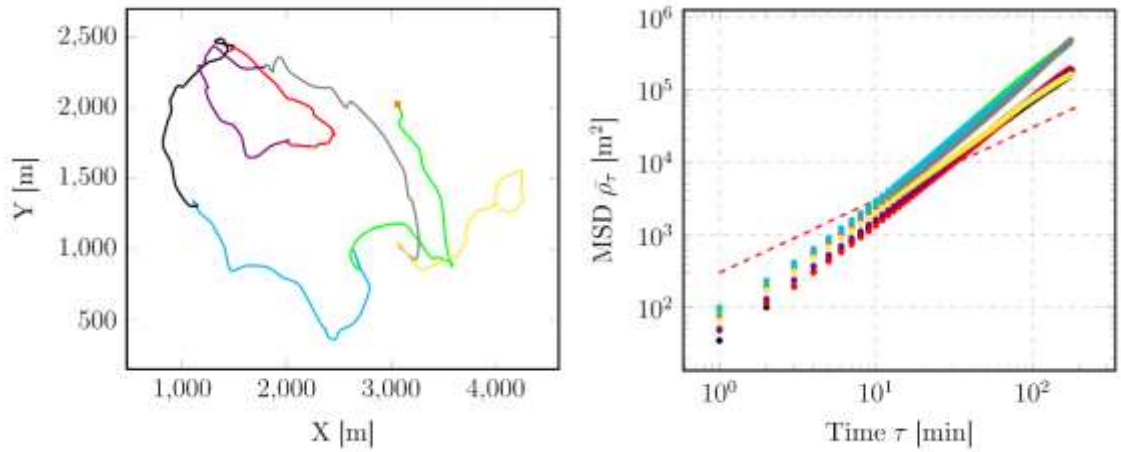

738

739 *Fig. S1 – Evolution of the troop position (left), with the corresponding mean squared displacements (MSDs, right,*
740 *mean α = 1.69 +- 0.08) for a tracking of 7 consecutive days during high food availability in plantations. The orange*
741 *square indicates the departure of the troop and the dashed line represents a line of a unitary slope, i.e. for α = 1.*

742

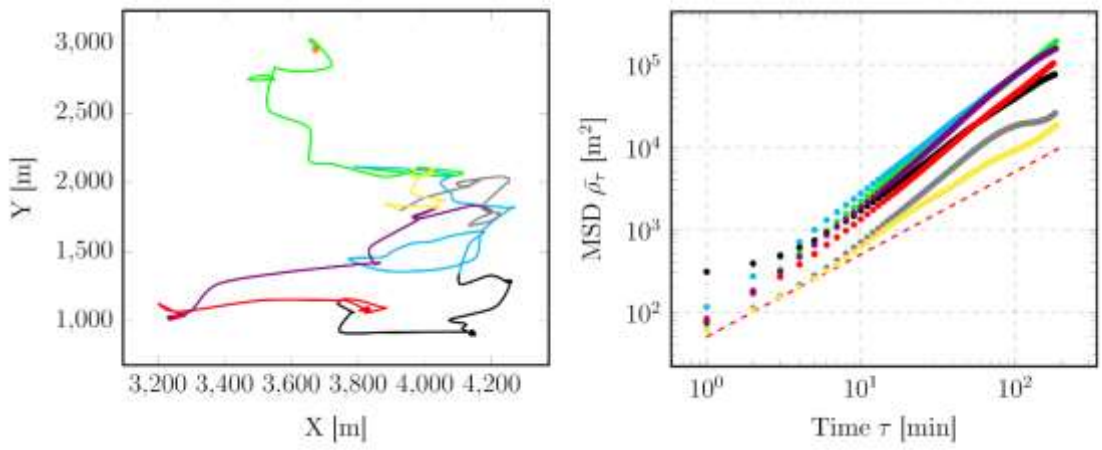

Fig. S2 – Evolution of the troop position (left), with the corresponding mean squared displacements (MSDs, right, mean α = 1.36 +- 0.15) for a tracking of 7 consecutive days during low food availability in dry evergreen forest and plantations. The orange square indicates the departure of the troop and the dashed line represents a line of a unitary slope, i.e. for α = 1.

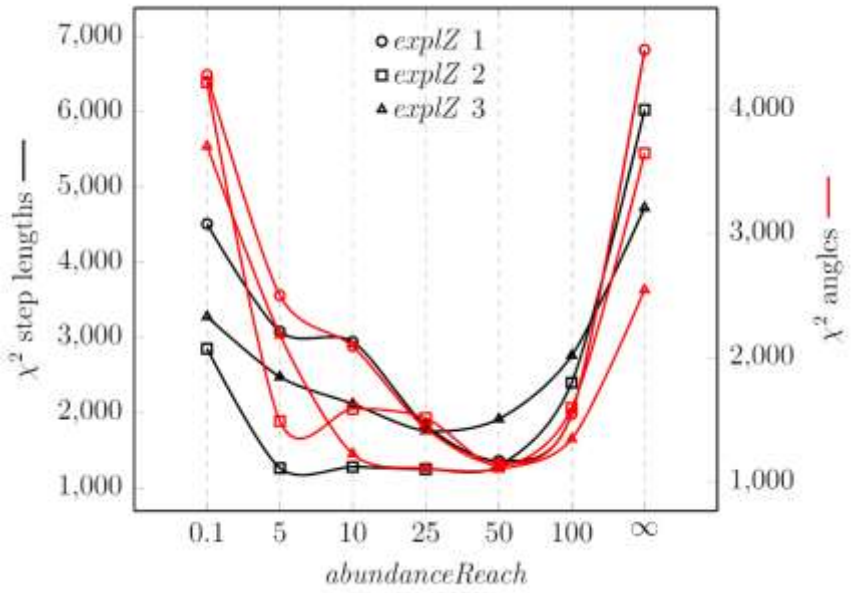

Fig. S3 – χ^2 for comparing step length and angle distributions between observed and simulated trajectories as a function of abundanceReach, for velocity = levyRatio = 1 and explorationZone = 1, 2 and 3. The black (resp. red) curves represent the χ^2 for step lengths (resp. angles) and are plotted along the left-hand (resp. right-hand) y-

axis. For each simulation, the group of particles was simulated from the same starting point and on a map of high food availability in plantations.

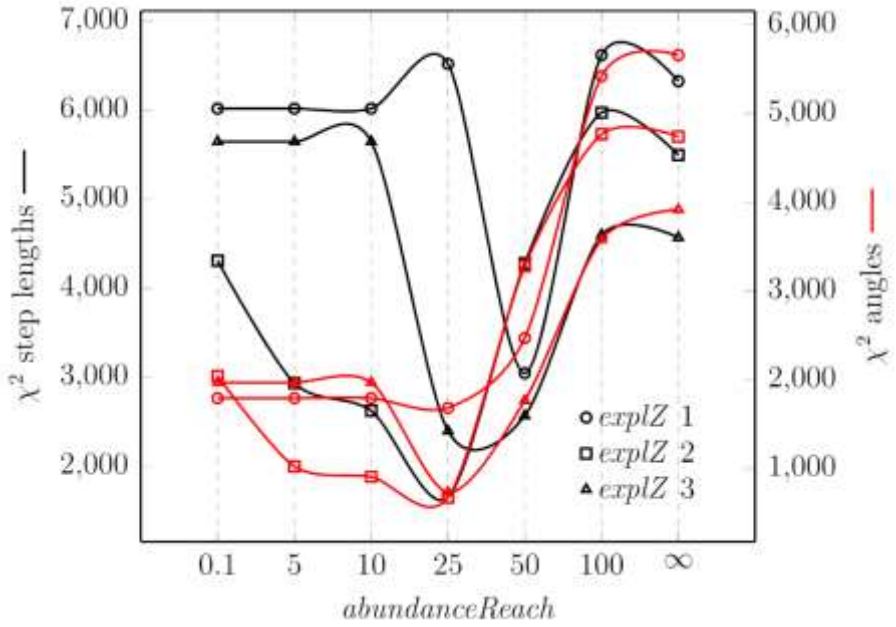

Fig. S4 – χ^2 for comparing step length and angle distributions between observed and simulated trajectories as a function of abundanceReach, for velocity = levyRatio = 1 and explorationZone = 1, 2 and 3. The black (resp. red) curves represent the χ^2 for step lengths (resp. angles) and are plotted along the left-hand (resp. right-hand) y-axis. For each simulation, the group of particles was simulated from the same starting point and on a map of low food availability in dry evergreen forest and plantations.

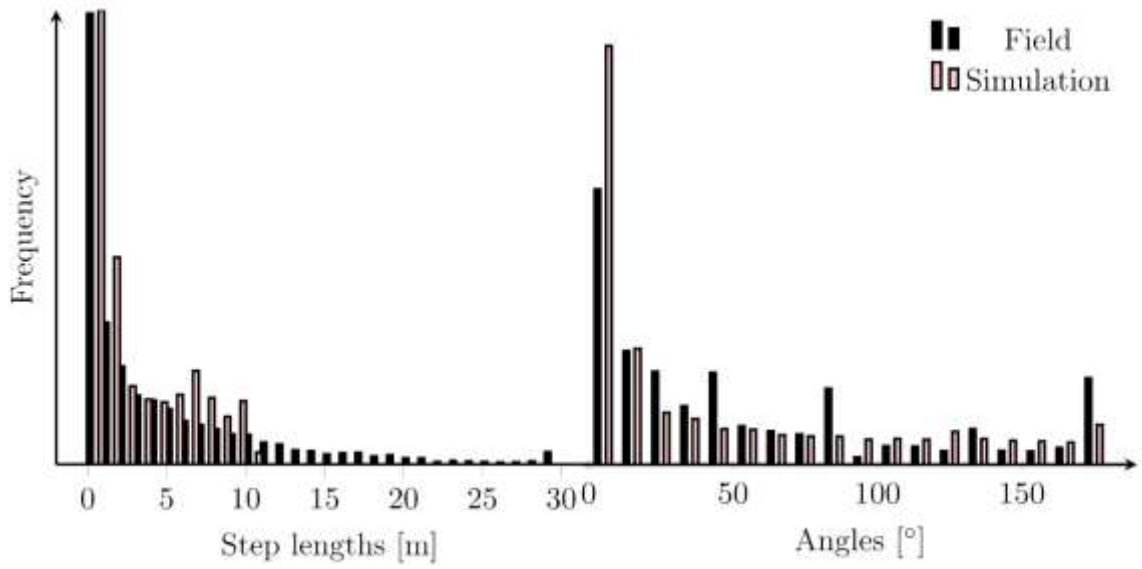

764

765 *Fig. S5 – Histogram of step lengths (left) and angles (right) for field (black) and simulation (red) data during high*
766 *food availability in plantations, with control parameters abundanceReach = 0.1, explorationZone = 2, velocity = 1*
767 *and levyRatio = 60. χ^2 = 1211 (resp. 1245) for step lengths (resp. angles).*

768

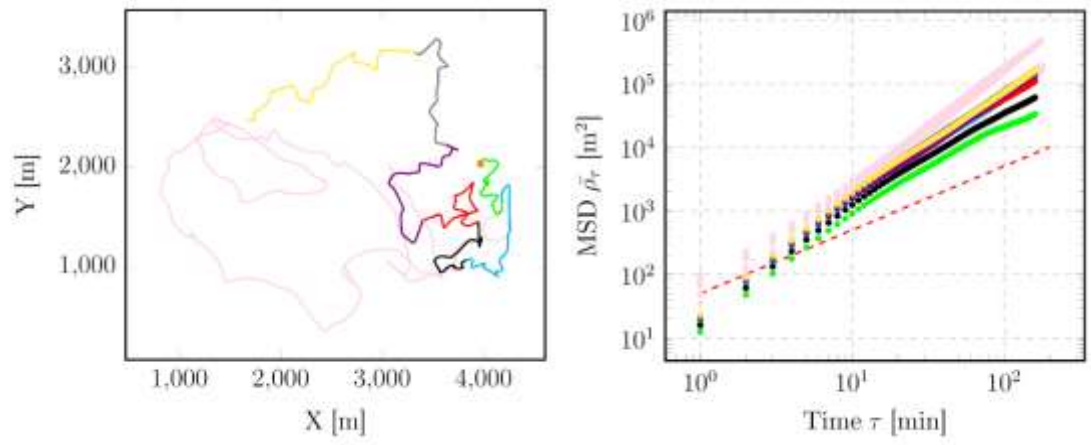

769

770 *Fig. S6 – Evolution of the group position (left), with the corresponding mean squared displacements (MSDs, right,*
771 *mean α = 1.56 +- 0.09) for a simulation of 7 consecutive days during high food availability in plantations, with*
772 *control parameters abundanceReach = 0.1, explorationZone = 2, velocity = 1 and levyRatio = 60. Pink trajectories*
773 *and MSDs represent the troop data. The orange square indicates the departure of the group of particles and the*
774 *dashed line represents a line of a unitary slope, i.e. for α = 1.*

775

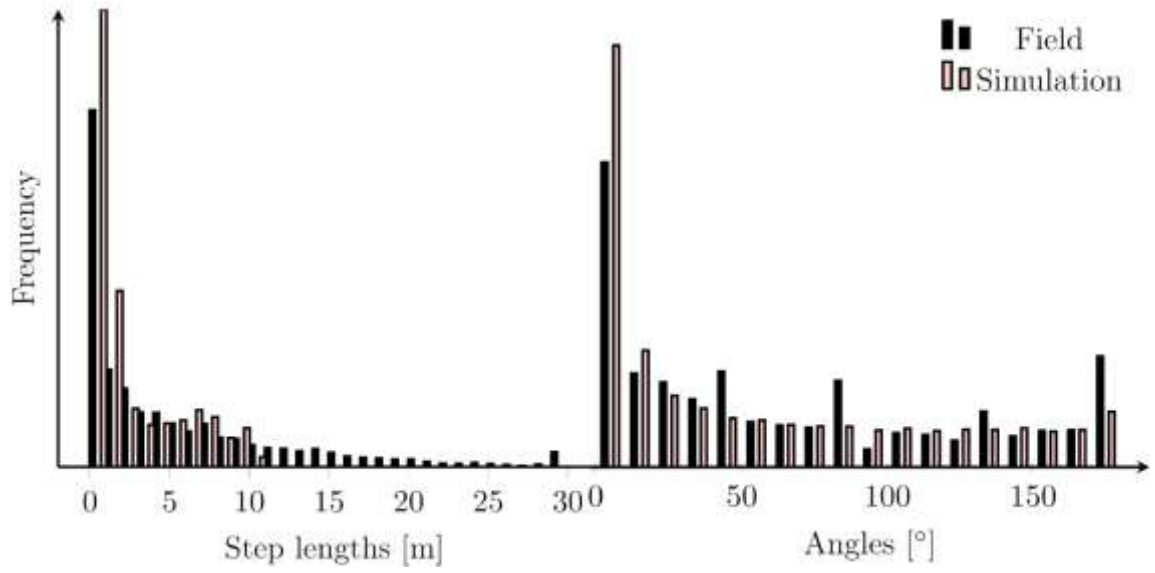

Fig. S7 – Histogram of step lengths (left) and angles (right) for field (black) and simulation (red) data during low food availability in dry evergreen forest and plantations, with control parameters abundanceReach = 0.1, explorationZone = 2, velocity = 1 and levyRatio = 35. χ^2 = 1419 (resp. 538) for step lengths (resp. angles).

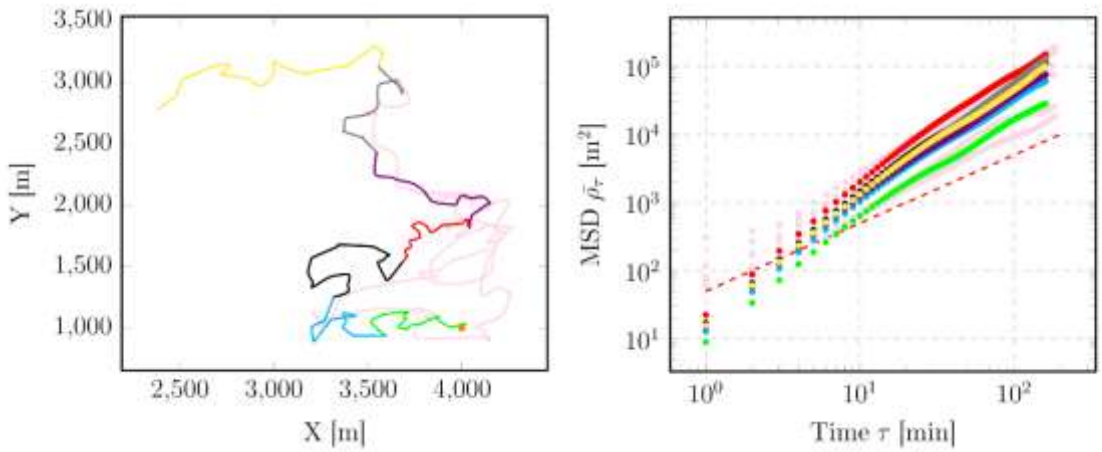

Fig. S8 – Evolution of the troop position (left), with the corresponding mean squared displacements (MSDs, right, mean α = 1.57 +- 0.06) for a simulation of 7 consecutive days during low food availability in dry evergreen forest and plantations, with control parameters abundanceReach = 0.1, explorationZone = 2, velocity = 1 and levyRatio = 35. Pink trajectories and MSDs represent the troop data. The orange square indicates the departure of the group of particles and the dashed line represents a line of a unitary slope, i.e. for α = 1.

Supplementary Files

This is a list of supplementary files associated with this preprint. Click to download.

- FigS1.pdf
- FigS2.pdf
- FigS3.pdf
- FigS4.pdf
- FigS5.pdf
- FigS6.pdf
- FigS7.pdf
- FigS8.pdf
- VideoS1.mov
- VideoS2.mov